Bosch, W., Savcenko, R., Flechtner, F., Dahle, C., Mayer-Gürr, T., Stammer, D., Taguchi, E., Ilk, K. H. (2009): Residual ocean tide signals from satellite altimetry, GRACE gravity fields, and hydrodynamic modelling. - Geophysical Journal International, 178, 3, pp. 1185—1192.

DOI: http://doi.org/10.1111/j.1365-246X.2009.04281.x

Geophys. J. Int. (2009) **178,** 1185–1192 doi: 10.1111/j.1365-246X.2009.04281.x

FAST TRACK PAPER

Residual ocean tide signals from satellite altimetry, GRACE gravity fields, and hydrodynamic modelling

Wolfgang Bosch,[1] Roman Savcenko,[1] Frank Flechtner,[2] Christoph Dahle,[2] Torsten Mayer-Gürr,[3] Detlef Stammer,[4] Eifu Taguchi[4] and Karl-Heinz Ilk[3]

[1]*Deutsches Geodätisches Forschungsinstitut (DGFI), München, Germany. E-mail: bosch@dgfi.badw.de*
[2]*GeoForschungsZentrum Potsdam (GFZ), Potsdam, Germany*
[3]*Institut für Geodäsie und Geoinformation (IGG), University Bonn, Germany*
[4]*Institut für Meereskunde (IfM), University Hamburg, Germany*

Accepted 2009 June 3. Received 2009 June 3; in original form 2009 February 2

SUMMARY

Improvements of a global state-of-the art ocean tide model are identified and quantified by applying three independent approaches, namely (i) empirical ocean tide analysis of multimission altimeter data, (ii) evaluation of GRACE data and gravity field models and (iii) high resolution hydrodynamic modelling. Although these approaches have different capabilities to sense ocean tides they obtain results which are basically consistent one with each other. The analysis of altimeter data clearly identifies significant residual amplitudes over shallow water for all major diurnal and semidiurnal constituents and the non-linear tide M_4. GRACE data and the time-series of monthly gravity field models exhibit—on a larger scale—residual ocean tide signals over much the same areas. The analysis of dynamic residuals of hydrodynamic modelling with data assimilation proves the validity of linear dynamics in the deep ocean and shows correlation of dynamic residuals with energy dissipation in these areas.

Key words: Time series analysis; Numerical solutions; Inverse theory; Space geodetic surveys; Time variable gravity; Tides and planetary waves.

1 INTRODUCTION

Prediction of ocean tides is crucial for the coastal environment and the protection of its ecosystem. However, knowledge of ocean tides is also needed for the proper treatment of space observation analysed, for example, to compute satellite orbits, to determine the Earth gravity field or to map and monitor the ocean surface. For example, the effect of ocean tides has to be removed from CHAMP, GRACE and GOCE observations in order to obtain gravity field models describing exclusively the Earth gravity. Altimetric sea surface heights are to be de-tided in order to allow studying smaller, non-tidal signals and to allow assimilation into numerical models.

In deep ocean the ocean tides are assumed to be known to within 2 cm root-mean-square (rms) uncertainty at wavelengths of 50 km (Shum *et al.* 2001). However, over continental shelves and in polar oceans much larger deficiencies for ocean tides are well known—even for the most recent models. Already 1999 Andersen showed the capability of the TOPEX altimeter system to improve the ocean tide signal in the European shelf region. Relative to FES2004 (Lyard *et al.* 2006), one of the most recent global ocean tide models, Savcenko & Bosch (2007) identified in the same area significant residual tide signals by a common analysis of multimission altimetry data. In the Atlantic Ocean, Ray (private communication, 2007) compared the overtide M_4 with ground truth and found rms differences significant smaller than with FES2004. King & Padman (2005), Han *et al.* (2005) and Han *et al.* (2007) showed that in Antarctica state-of-the-art ocean tide models have significant S_2 and M_2 errors, due to poor or missing altimetry and lack of tide data at high latitudes. Padman & Fricker (2005) use ICESat data to compare the accuracy of several ocean tides models over the Ross Ice Shelf.

Deficiencies in global ocean tide models are also a severe concern for the gravity field modelling by GRACE. Wünsch *et al.* (2005) showed that the differences of two state-of-the-art ocean tide models may partly explain the artificial striping still present in the latest models. Following Knudsen & Andersen (2002) the GRACE alias frequencies for S_2 and K_2 are much longer than 30 d leaving the errors of these constituents almost unreduced in monthly gravity field solutions. Moore & King (2008) also quantify tidal aliasing of GRACE over Antarctica and state that constituents K_1, K_2 and S_2 with long alias periods potentially compromise long-term variability studies. Seo *et al.* (2008) estimate GRACE alias errors taking the differences of GOT00.2 and TPXO6.2 as a proxy for tidal errors.

This paper compiles results of different approaches performed to achieve considerable improvements over a state-of-the-art ocean tide model by (i) applying harmonic analysis to multimission altimeter data on a dense, nearly global grid, (ii) analysing the GRACE

K-band range data residuals and monthly gravity fields indicating regions where the ocean tide model is inadequate and (iii) hydrodynamic modelling on a dense grid with assimilation of tidal constituents from tide gauges and altimetry.

2 RESIDUAL TIDE ANALYSIS FROM MULTIMISSION ALTIMETRY

Satellite altimetry is corrected for ocean tides in order to allow the study of smaller, non-tidal signals. However, altimetry observation itself can be used to empirically analyse ocean tide constituents. This was already demonstrated by many investigations, for example, by Cartwright & Ray (1990), Schrama & Ray (1994), Andersen (1999), Ray (1999) and others. The ocean tide analysis by altimeter data suffers from the rather sparse sampling of the high frequency tidal signal. As altimeter satellites repeat their observations approximately only every 10 (TOPEX or Jason1), 17 (Geosat and GFO), or even 35 d (ERS, ENVISAT), diurnal and semi-diurnal tidal signals become visible only as signals with rather long periods. Smith (1999) investigated in detail the alias periods of different altimeter satellites.

With about 10 yr TOPEX provided an exceptional long time-series of observations along its original ground track. Jason1 (and since short time Jason2) continues to observe the same ground track. These time-series allow resolving and decorrelating all major tidal constituents. However, with an equatorial ground track spacing of more than 300 km the spatial resolution of TOPEX and Jason1 is inadequate for observing ocean tides in shallow regions. After the cross calibration with Jason1 the ground tracks of TOPEX were shifted such as to double the spatial resolution. On the new ground tracks TOPEX continued its observations another 3 yr, a period still sufficient to estimate most of the tidal constituents. The ESA missions, ERS-1/2 and ENVISAT, provide an even denser ground track pattern with a spacing of 80 km. However, the high spatial resolution can't be fully exploited as the sun-synchronous orbits of these missions do not at all allow estimating solar constituents such as, for example, S_2. For other constituents to be resolved and separated the 35 d repeat period of the ESA missions requires a particular long time-series. M_2 and N_2, for example, can be separated only after 8.5 yr (see Smith 1999, for details), an observation period, requiring a consistent concatenation of ERS-2 and ENVISAT data.

The combination of data from consecutive missions or missions with different sampling characteristics was performed at the Deutsche Geodätische Forschungsinstitut (DGFI) and allows mitigating the obstacles of individual missions. Combining data from different mission in a common tide analysis requires, however, a careful upgrading, harmonization and cross calibration. Upgrading was realized at DGFI by replacement of new orbits (for the ESA missions), time tag corrections (for ERS-1/2) and improved correction models for the microwave radiometer (TOPEX). Harmonization implies to use as far as possible the same correction models. For example, for all missions the inverted barometer correction was replaced by the dynamic atmospheric corrections (DAC) produced by CLS Space Oceanography Division using the MOG2D model from LEGOS (Carrère & Lyard 2003). Moreover, the ocean tide corrections for all missions were based on the FES2004 (Lyard *et al.* 2006). Finally, the cross calibration was performed by a global crossover analysis based on nearly simultaneous single- and dual-satellite crossover differences performed between all altimeter systems operating contemporaneously. This crossover analysis captures not only relative range biases, but also systematic inconsistencies in the centre-of-origin realization and geographically correlated errors. For the details of this multimission cross calibration see Bosch & Savcenko (2006).

As all altimeter data is already corrected by the FES2004 ocean tide model a harmonic analysis is performed by estimating simultaneously mean value, trend, seasonal variations (annual and semi-annual periods), and residuals to the tidal constituents M_2, S_2, K_2, N_2, Q_1, P_1, K_1, O_1, $2N_2$ and to the non-linear tidal constituent M_4. To mitigate the correlation problems the analysis is performed on a global, regular geographical $15' \times 15'$ grid. For every grid node normal equations are accumulated using all measurements from all altimeter systems inside a spherical cap. In shallow water (depth less than 200 m) the cap radius was set to 1.5° and a Gauss function with half weight width of 0.5° is applied for weighting inverse proportional to the distance. Over the deep ocean a cap radius of 4.5° and half-weight width of 1.5° are used. First attempts of this analysis are described in Savcenko & Bosch (2007), the final results have been compiled to a new empirical ocean tide model EOT08a (Savcenko & Bosch 2008).

The panels in Fig. 1 indicate an area in South East Asia with rather outstanding results for the residual amplitudes. In shallow water areas the semidiurnal constituents M_2 and S_2 exhibit numerous pattern with significant residuals with amplitudes up to 15 cm. N_2 and K_2 as well as the diurnal constituents Q_1, P_1, K_1, O_1 and the non-linear shallow water tide M_4 can take residual amplitudes up to 5 cm. There are also long wavelength pattern with residual amplitudes of a few centimetres. Even the weakest tidal constituent $2N_2$ exhibit residual amplitudes of 2 cm in the Yellow Sea.

As described in detail in Savcenko & Bosch (2008), EOT08a was carefully validated by (i) the reduction in variance of altimeter time-series at crossover points (see the example in Fig. 2) and (ii) historical bottom pressure records from BODC, available on the Northwest European Shelf. Comparisons with the constants of pelagic tide gauges (Smithson 1992), a few additional ocean bottom pressure records and the ST102 data set (Ray, private communication, 2007) were also carried out to validate the improvements against the FES2004 reference model. The separability of tidal constituents is satisfactory as the global mean of correlations between critical constituents (e.g. S_2 and mean value, or K_2 and Ssa) remains below 0.3.

3 OCEAN TIDE SIGNALS IN GRACE GRAVITY FIELD SOLUTIONS AND INSTRUMENT DATA

At the GeoForschungsZentrum (GFZ), Potsdam, and the Institute for Geodesy and Geoinformation (IGG, formerly ITG), Bonn, nearly the complete GRACE mission data have recently been reprocessed based on updated background models and processing standards. These time-series are called EIGEN-GRACE05S (Schmidt *et al.* 2008) and ITG-GRACE03S (Mayer-Gürr *et al.* 2007b, details can be found for the previous solution at Mayer-Gürr *et al.* 2007a), respectively, and are provided to the user community in terms of monthly sets of spherical harmonic coefficients to be used for monitoring of time-varying geophysical phenomena in the system Earth. For the interpretation of the residual (monthly minus long-term mean) signal various known time-variable gravity effects are already reduced from the GRACE data in the course of the adjustment process. These comprise, for example, the gravity signals induced by the third-body accelerations on the satellites and

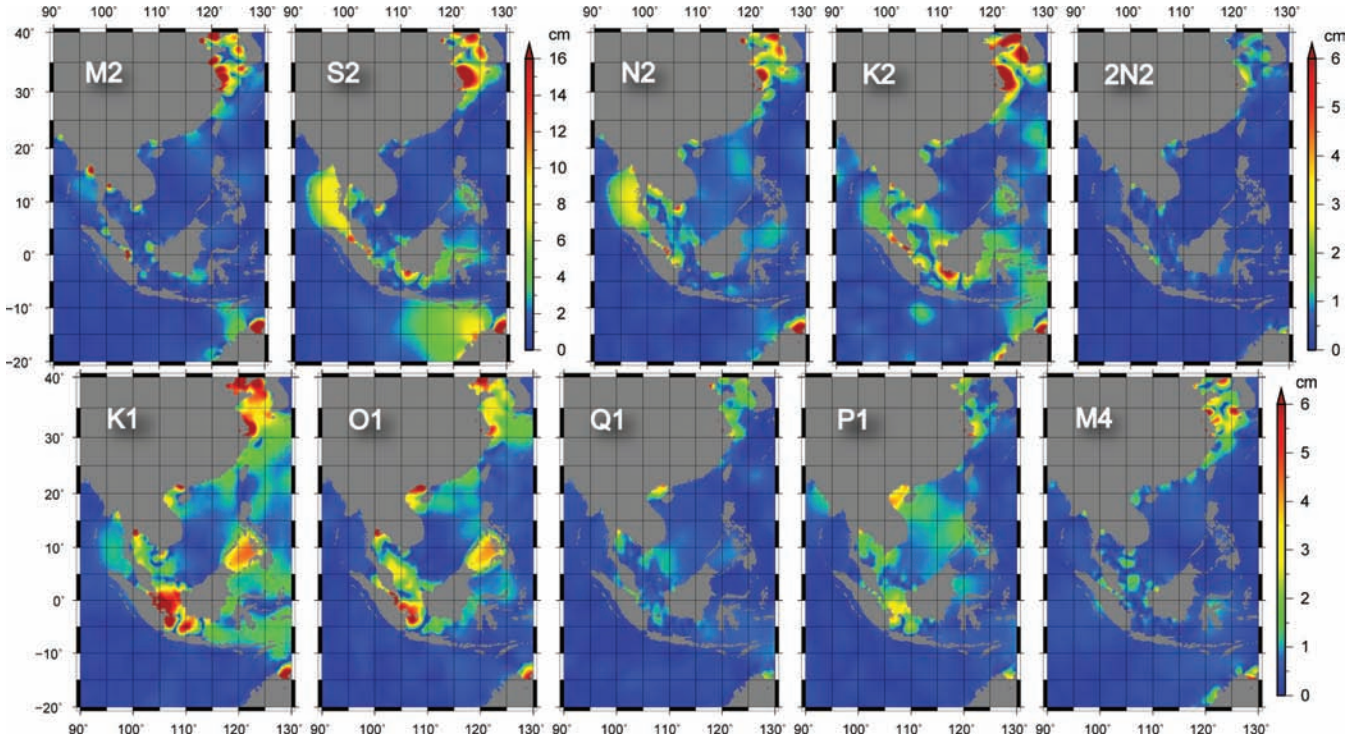

Figure 1. Residual amplitudes (cm) of the semidiurnal constituents M_2, S_2, N_2, K_2 (top row panels) and of the diurnal constituents K_1, O_1, Q_1, P_1 and the shallow water constituent M_4 (bottom row panels). The amplitudes are residuals with respect to the FES2004 model, a standard model used to correct all altimetry data. For M_2 and S_2 there are areas with residuals up to or even above 15 cm. Note, the colour scale for M_2, S_2 is different compared to the colour scales for the other constituents, showing residual amplitudes up to 5 cm. Beside extreme residuals showing up in shallow water there are also areas with considerable extension with rather uniform residuals of 3–5 cm (e.g. for S_2 northwest of Australia) or 1–2 cm (for P_1 in the South China Sea).

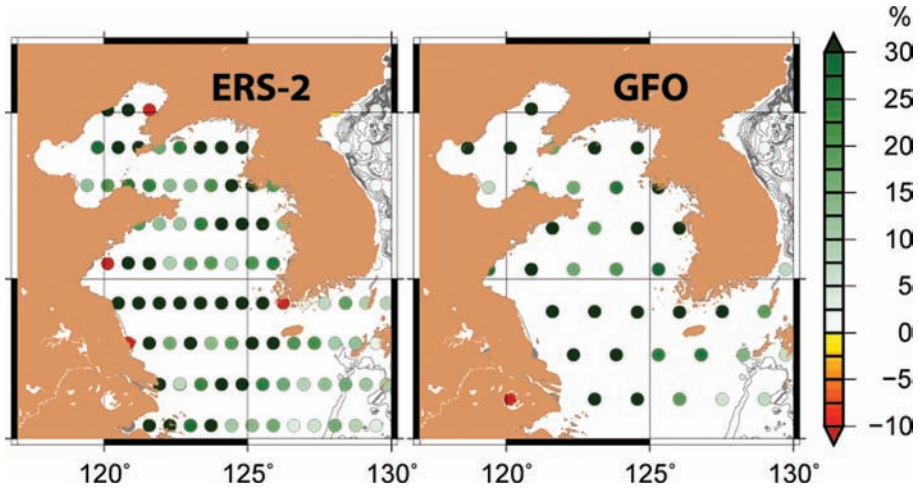

Figure 2. Percentage gain in variance of altimeter time-series at crossovers of ERS-2 (left-hand panel) and GFO (right-hand panel) achieved after applying the residual tide corrections estimated for EOT08a. The area shown is the Yellow Sea, characterized in Fig. 1 by the most outstanding residual amplitudes.

the Earth due to the gravitational pull from the Sun, the Moon and planets, gravity variations from short-term (non-tidal) mass redistributions in the atmosphere and the oceans, secular gravity changes in selected long-wavelength gravity coefficients due to the global isostatic adjustment as well as the pole tide effect on the solid Earth and the oceans caused by the variations in the Earth's rotation. Finally, the luni-solar tides of the solid Earth, the oceans and the atmosphere (inclusive the indirect effects from loading and deformation due to the change in the mass distribution) are corrected by appropriate models. For the ocean tides, as for the altimetric approach described above, the FES2004 model is applied. Consequently, the residual gravity signal derived from the GRACE monthly models should mainly represent unmodelled effects from hydrology, post glacial rebound or mass changes of the polar and Greenland ice caps and inland glaciers.

The temporal effects due to ocean tides are assumed to be precisely known during gravity field determination and that they could be removed using current models. However, Han *et al.* (2004) have already shown in a simulation study that model errors in S_2 cause errors three times larger than the GRACE measurement noise

below degree 15 of the monthly GRACE gravity solutions. Wünsch *et al.* (2005) compared two different ocean tide models with respect to GRACE data analysis and found significant errors for S_2 and M_2, for example, in Antarctica which are due to poor or missing altimetry and tide data at high latitudes. The differences of nine short-periodic tides show the typical GRACE related meridional north–south striping as well as a strong signal in the Weddell Sea. Ray & Luthcke (2006) concluded in their analysis that the accepted GRACE error budget is roughly one order of magnitude larger than the component arising from tide modelling errors. Meanwhile, with the latest reprocessed solutions this is not true anymore because the calibrated errors of these reprocessed solutions are now much below the values assumed in the 2006 study and already touch the simulated tide error curve at long wavelengths.

In practice, Han *et al.* (2005) already extracted M_2 and S_2 ocean tides underneath the Filchner–Ronne and Larsen ice shelves from time-series of regional GRACE gravity fields and found a good agreement for a spatial resolution of 300 km with predicted tides of the FES2004 model. To manifest the capability of GRACE for ocean tide analysis two different experiments have been performed at GFZ and ITG.

Fig. 3 (top panel) shows the cosine signal of the 161 d (the alias period of the S_2 ocean tide) fit of GFZ's EIGEN-GRACE05S monthly gravity field solutions between 2002 August and 2007 July up to degree and order 60 (without C_{20} and smoothed with a Gaussian filter of radius 500 km). Only 5 out of 60 months are missing due to, for example, GRACE instrument data problems. Three kinds of signals can be detected. First, typical meridional-oriented spurious gravity signals ('stripes'), most likely due to the GRACE north–south oriented orbital ground tracks and the subsequent pure along-track sampling of the K-band SST instrument, insufficient instrument data parametrization or deficiencies in the background modelling such as for ocean tides (see above). Second, two strong and hard to separate hydrological related semi-annual signals in the Amazon region. Finally, several peaks with amplitudes of about 3 cm height of an equivalent mass of water in the Indonesian shelf region, the East Chinese and in the Weddel Sea which are also reported—with slightly larger amplitudes—in Melachroinos *et al.* (2009).

In contrast to GFZ's gravity field analysis, IGG has directly investigated the GRACE instrument data using FES2004 and EOT08a to correct for ocean tides. Here, 4.5 yr of K-band residual range-accelerations between 2002 August and 2007 April have been analysed for each global $2^\circ \times 2^\circ$ grid cell using EIGEN-GRACE05 similar background models and standards. For each cell an individual harmonic analysis of the respective time-series of residuals has been performed and the amplitudes and phases of different partial tides have been adjusted. Fig. 3 (middle panel) shows exemplarily the result for M_2 when using FES2004. The strongest residual signal is detected in the shelf areas along the coastlines, but on the open ocean a significant signal is observed as well. Fig. 3 (bottom panel) depicts the amplitudes when EOT08a is applied. It becomes obvious that most of the residuals decrease or even disappear. Also note that the M_2 FES2004 deficiencies are located at similar locations than detected for S_2 at GFZ when analysing gravity field time-series. Also, both results from GFZ and IGG show the strong peak in the Weddell Sea observed by Wünsch *et al.* (2005). Additionally, these artefacts are highly correlated with errors in the FES2004 model as derived from altimetric analysis (see Fig. 1) and thus confirm the potential of the GRACE mission to observe long-wavelength ocean tides.

4 DATA ASSIMILATION FOR OCEAN TIDES WITH DYNAMIC RESIDUAL ANALYSIS

Empirical tide models (Ray 1999; Savcenko & Bosch 2008) have reached high performance in reproducing the tidal constants of sea surface elevations for major diurnal and semi-diurnal tides overall in the deep oceans. Even so there are some reasons to incorporate efficient numerical data assimilation models. Firstly, appearance of non-linear short waves in shallow waters limits possibilities of the empirical analysis method (Andersen 1999). Secondly, in geophysical applications tidal currents play a substantial role in investigating tidal dissipation/mixing and associated meridional overturning circulation. They are computed commonly by use of numerical hydrodynamic models with/without data assimilation. Fourthly, due to the limited coverage of satellite altimetry the North and the South Pole are difficult regions to recover the tidal dynamics without numerical models. Finally, physical validation of the empirical data is also needed.

Since the late 1980s a generalized inverse method for tide modelling has been developed at the University of Hamburg, now called Hamburg direct data Assimilation Methods for TIDEs (HAMTIDE). The approach is somewhat related to the representer method (Bennett 1992), but the way of solution is quite different: the HAMTIDE solution is obtained by direct minimization of the model-data misfit in a least square sense, requiring to compute the least square solution as an over determined system of linear algebraic equations. The Laplace tidal equations are converted into linear spectral elliptic differential equations forced by the tide generating potential of degree 2. The dynamic residuals are used for the detection of possible model errors, such as bathymetry and parametrization of dissipation (Zahel 1995; Egbert 1997).

HAMTIDE is close to the spectral linearized hydrodynamic model CEFMO and the associated data assimilation model CADOR (Lyard *et al.* 2006). Main difference of both models is that the HAMTIDE model is characterized by a specific way to consider dynamic error covariances consisting in the addition of spatial derivatives of the dynamic residuals to the cost function. This procedure corresponds to the adoption of a Gaussian error covariance matrix for the model errors. The associated smoothing leads to physically interpretable residual fields (Zahel *et al*. 2000). The loading and self-attraction (LSA) effect caused by redistribution of water and seafloor is taken into account in HAMTIDE by applying the full Love number approach (CLSA) or by parametrizing LSA that includes a term proportional to the local tidal elevation (PLSA; Zahel 1991).

For the present analysis, the HAMTIDE model is run with 10' spatial resolution. The solution is constrained exclusively by data taken from the DGFI altimeter data bank EOT08a being explained in part 2. Data are allocated on to the elevation points of Arakawa C-grids at every 2° between $+66^\circ$ and -66° for data assimilation. In pole regions up to $\pm 74^\circ$ data are arranged in every 3° and specially over Northwest European and Patagonian Shelves data are distributed in every 1°. As a whole, 9006 assimilation data are used to obtain over 3 million control variables. For the energy dissipation depth dependent bottom friction and varying eddy viscosity parameters with latitude are used. The PLSA is adopted to allow for the secondary potential due to LSA, simply because results using CLSA do not differ substantially from those using PLSA in models with data assimilation (Zahel 1991), and for the sake of computational economy. The HAMTIDE results are compared to a reference pelagic data set ST102p (Ray, private communication, 2007). The

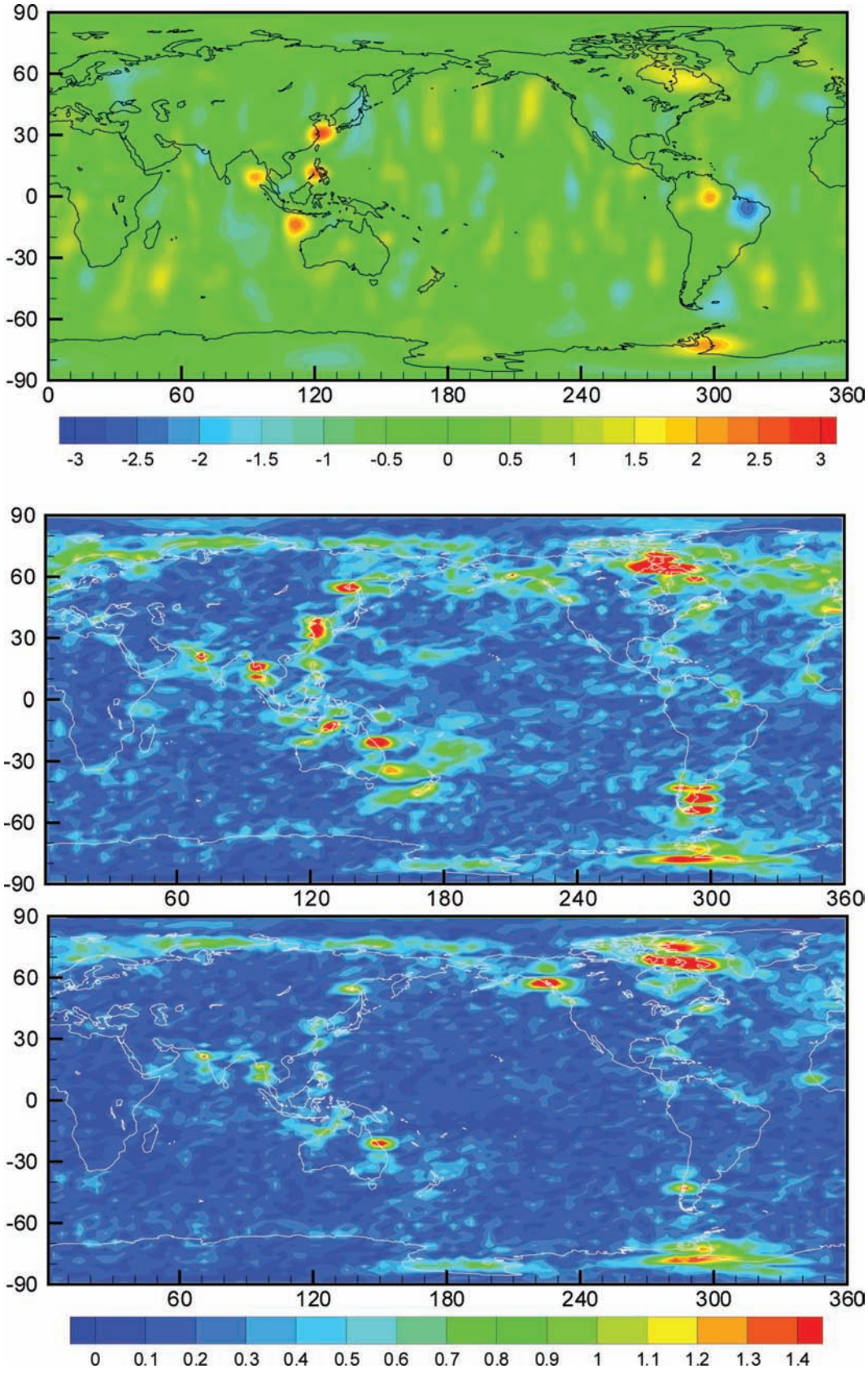

Figure 3. Top panel: Cosine signal of the 161 d fit (aliasing period of S_2) of GFZ EIGEN-GRACE05 monthly gravity field solutions between 2002 August and 2007 July up to degree and order 60 (without C_{20}, smoothed with Gaussian filter of radius 500 km) expressed in terms of the height of an equivalent mass of water in cm. Middle: Harmonic analysis for M_2 of residual GRACE K-band range-accelerations for $2^\circ \times 2^\circ$ global grid cells using 4.5 yr of ITG-GRACE03S data between 2002 August and 2007 April with FES2004 as background model expressed in nm s^{-2}. Bottom panel: same as before using EOT08a instead of FES2004.

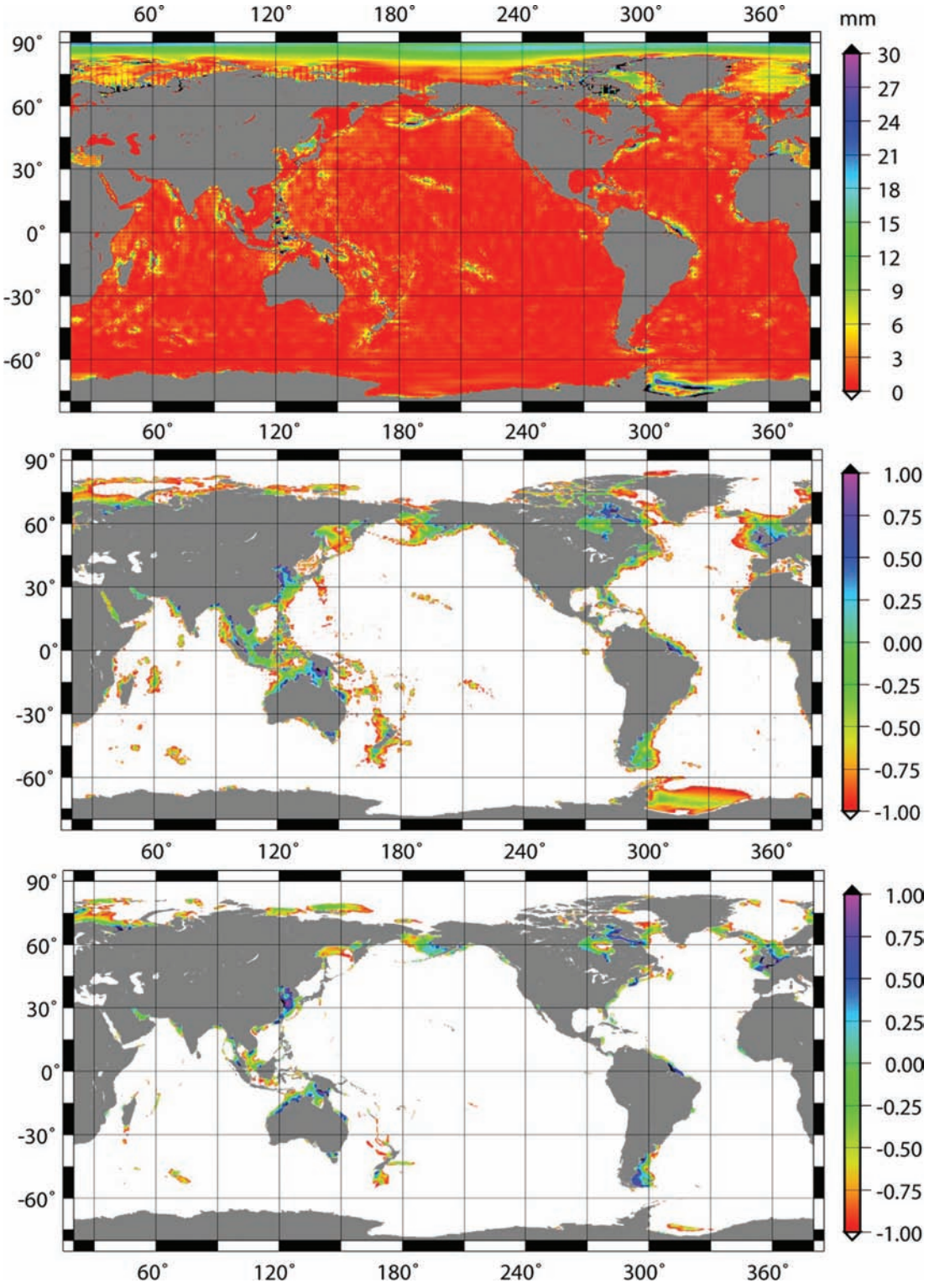

Figure 4. Top panel: rms differences between HAMTIDE and EOT08a models (in mm) for M_2. Middle panel: Log_{10} of normalized rms magnitudes of dynamic residual vectors, normalized by a global rms mean value. Bottom panel: Log_{10} of normalized rms magnitudes of linear friction energy vectors, normalized by a global rms mean value.

rms differences of eight major tide constituents (M_2 S_2, N_2, K_2, K_1, O_1, Q_1 and P_1) in the complex plane are agreeing to FES2004 to a large extent. rms differences between HAMTIDE and EOT08a are shown in Fig. 4 for the M_2 constituent (top panel). They are small (0.3 cm) in the open ocean (>1000 m), but rather large (4.2 cm) in shallow water regions (<1000 m) between 66°N and 66°S. Clearly, both tidal fields suffer from inaccuracies in North and South Polar Regions, due to the lack of accurate elevation and bathymetry data, but also ignoring ice shelf dynamics in present model. Discrepancies occur also near areas of steep topographic slopes, including

continental margins (e.g. south of Aleutian Chain, southeast of New Scotland, Ross and Weddell Seas) and sea mounts (e.g. Mauritius, Hawaii and Marquises Islands), where the numerical model cannot catch rapid spatial change in the sea bottoms. On the other hand induced fluctuations of the sea height may give rise to anomalous altimetry.

The close agreement of numerical and empirical models in the deep ocean is reflected in the middle panel of Fig. 4, showing the normalized rms magnitudes of dynamic residual vectors. The small residual implies the validity of making use of the linear dynamics in the deep ocean and can be also deduced that the empirical model satisfies the hydrodynamics as well. The high correlation between dynamic residuals and the dissipation by linear bottom friction in the shallow water regions (e.g. Patagonian shelf, Hudson Bay, Northwest European Shelf, Indonesian Waters, the shelf areas northwest of Australia, Yellow Sea, Weddell Sea and some other coastal and island regions in Fig. 4, middle and bottom panels) is not surprising. Missing non-linear effects are corrected effectively by the data and consequently by the dynamic residuals as forcing. The energy conversion through advection terms into higher harmonics can occur in the mentioned areas and the full non-linear data assimilation scheme (Taguchi 2004) should be implemented for selected shelf regions, where over and compound tides cannot be neglected. Even in some deep-sea regions, like in the Atlantic Ocean, M_4 could play a significant role due to the radiation from shelf areas (Ray 2007).

As every numerical model approximates the hydrodynamic equations differently, the data induced dynamic residuals vary from model to model. In comparison to the output of Zahel *et al*. (2000), the maximums of the residuals in the current work are concentrated to a highest extent near the coastlines (Fig. 4, middle), implying more corrections of the dynamics (mainly for linear friction terms) having taken place there. Particularly, a relative maximum of the residuals, appearing in the above 1°-model south of Australia due to using an inadequate bathymetry of the Southern Ocean in the 1°-model, now disappears in the actual high resolution model, characterized by an adequate bathymetry. The maximum of the residuals in the 1°-model is connected with an unrealistic amphidrome, which is typical of data-free models with lower spatial resolution, and does neither arise in global models with data assimilation, nor in high-resolution data-free models with an adequate bathymetry. Substantial dynamic residual energy is consumed (39 per cent of the total dissipation 2.42 TW being computed by the current model) near trenches, ridges and continental slopes, possibly for the conversion of barotropic tidal energy into internal waves (Egbert & Ray 2000). As was explained by Lyard *et al.* (2006) and by Zaron & Egbert (2006), the baroclinic conversion energy due to internal tide drags could be parametrized in several ways, and dynamic residuals can be reduced greatly by incorporating one of those formulations. Dynamic residuals in HAMTIDE are determined by errors in paramerization of bottom friction, eddy viscosity, LSA and mainly by baroclinic energy conversion in the deep oceans. The last issue was found by comparison between dynamic residual energy in HAMTIDE and conversion energy over 20 selected patches in Simmons *et al.* (2004). Agreements of both values to a large extent imply the identification of the conversion and the residual energy. Dynamic residuals thus compensate the missing form drags and may help to understand unknown tidal dissipations. At last, noticeable dynamic residuals are present in the whole Weddell Sea. Missing physics, for example, ice shelf dynamics in Ronne Ice Shelf, which are, unlike to FES2004 (Lyard *et al.* 2006), not present in the HAMTIDE model, and may cause biased M_2 tidal resonance and consequently large residuals. Details of above mentioned dynamic residuals would be further discussed in future.

5 CONCLUSIONS

The empirical ocean tide analysis of multimission altimeter data identifies and quantifies significant residual ocean tide signals relative to FES2004, a state-of-the-art model widely used in altimetry and gravity field processing. In shallow water areas the M_2 and S_2 constituents show numerous extended patterns with residuals taking amplitudes of up to 15 cm. Other major constituents and the non-linear shallow water tide M_4 hit residual amplitudes up to 5 cm. Validation at altimeter crossovers and with independent bottom pressure data confirm these findings. A correlation analysis proves the separability of the analysed constituents.

S_2 and M_2 ocean tide signals in GRACE instrument data and monthly gravity field solutions show peaks at similar locations as detected by the residual tide analysis from multimission altimetry. The high correlation proves the potential of GRACE to observe long-wavelength ocean tide errors.

The reproduction of partial tides is well established for both, linear inverse model (HAMTIDE) and data processing (EOT08a), especially in the deep ocean. This is demonstrated by the analysis of the dynamic residuals and by small deviations of the rms difference between them. However, relatively large rms differences against ST102p data set over rough topographies with high-energy dissipation by the dynamic residuals suggest needs to incorporate some forcing term in the equation systems to take the baroclinic energy conversion into account. The model deficiency introduced by neglecting non-linear terms is compensated by dynamic residuals to a large extent, meaning that assimilating data helps considering non-linear effects on the astronomical tidal constituents. However, the non-linear shallow water tides themselves are, of course, not resolved in the linear model. Non-linear terms like advection and quadratic bottom friction terms are not easy to implement in to the spectral model. Hence non-linear tides issue is moving to the time-stepping modelling (Arbic *et al.* 2004; Pairaud *et al.* 2008) and to modelling using statistical methods, for example, computational time saving empirical ensemble statistics (Mourre *et al.* 2004) Regarding this issue, a non-linear time-stepping HAMTIDE version will be implemented for selected shelf regions in the near future.

ACKNOWLEDGMENT

This work was funded by the Deutsche Forschungsgemeinschaft (DFG), Bonn, Germany, under the grants BO1228/5–1, FL592/2–1, IL 17/9–1, STA 410/12–1, and DFG06–419.

REFERENCES

Andersen, O.B., 1999. Shallow water tides in the northwest European shelf region from TOPEX/POSEIDON altimetry, *J. geophys. Res.,* **104**(C4), 7729–7742, doi:10.1029/1998JC900112.

Arbic, B.K., Garner, S.T., Hallberg, R.W. & Simmons, H.L., 2004. The accuracy of surface elevations in forward global barotropic and baroclinic tide models, *Deep-Sea Res. II,* **51,** 3069–3101.

Bennett, A.F., 1992. *Inverse Methods in Physical Oceanography,* Cambridge University Press, Cambridge, UK.

Bosch, W. & Savcenko, R., 2006. Satellite altimetry—multi-mission cross calibration, in *Dynamic Planet—Monitoring and Understanding*

a Dynamic Planet with Geodetic and Oceanographic Tools, Vol. 130, pp. 131–136, eds Tregoning, P. & Rizos, Ch., IAG Symposia, Springer, Berlin.

Carrère, L. & Lyard, F., 2003. Modeling the barotropic response of the global ocean to atmospheric wind and pressure forcing—comparisons with observations, *Geophys. Res. Let.*, **30**(6), 1275, doi:10.1029/2002GL016473.

Cartwright, D.E. & Ray, R.D., 1990. Oceanic tides from Geosat alimetry, *J. geophys. Res.*, **95**(C3), 3069–3090.

Egbert, D.D., 1997. Tidal data inversion: interpolation and inference, *Prog. Oceanog.*, **40,** 53–80.

Egbert, D.D. & Ray, R., 2000. Significant dissipation of tidal energy in the deep ocean inferred from satellite altimeter data, *Nature*, **405**.

Han, S.C., Jekeli, C. & Shum, C.K., 2004. Time-variable aliasing effects of ocean tides, atmosphere, and continental water mass on monthly mean GRACE gravity field. *J. geophys. Res.*, **109**(B4), B04403, doi:10.1029/2003JB002501.

Han, S.C., Shum, C.K. & Matsumoto, K., 2005. GRACE observations of M2 and S2 ocean tides underneath the Filchner-Ronne and Larsen ice shelves, *Geophys. Res. Lett.*, **32,** L20311, doi:10.1029/2005GL024296.

Han, S.C., Ray, R.D. & Luthcke, S.B., 2007. Ocean tidal solutions in Antarctica from GRACE intersatellite tracking data, *Geophys. Res. Lett.*, **34,** L21607, doi:10.1029/2007GL031540.

King & Padman, 2005. Accuracy assessment of ocean tide models around Antarctica, *Geophys. Res. Let.*, **32,** L23608, doi:10.1029/2005GL023901.

Lyard, F., Lefevre, F., Letellier, T. & Francis, O., 2006. Modelling the global ocean tides: modern insights from FES2004, *Ocean Dyn.*, **56,** 394–415, doi:10.1007/s10236–006-0086-x.

Knudsen, P. & Andersen, O., 2002. Correcting GRACE gravity fields for ocean tide effects, *Geophys. Res. Lett.*, **29**(8), 1178, doi:10.1029/2001GL014005.

Mayer-Gürr, T., Eicker, A. & Ilk, K.H., 2007a. ITG-Grace02s: a GRACE gravity field derived from short arcs of the satellites orbit, in *Proceedings of the 1st International Symposium of the International Gravity Field Sevice "Gravity Field of the Earth"*, Istanbul.

Mayer-Gürr, T., Eicker, A. & Ilk, K.H., 2007b. ITG-Grace03 gravity field model, www.geod.uni-bonn.de/itg-grace03.html

Melachroinos, S., Lemoine, J.M., Tregoning, P. & Biancale, R., 2009. Quantifying FES2004 S2 tidal model from multiple space-geodesy techniques, GPS and GRACE, over Northwest Australia, *J. Geod.*, doi:10.1007/s00190–009-0309–2.

Moore, P. & King, M.A., 2008. Antarctic ice mass balance estimates from GRACE: tidal aliasing effects. *J. geophys. Res.*, **113,** F02005, doi:10.1029/2007JF000871.

Mourre, B., De Mey, P., Lyard, F.L. & Le Provost, C., 2004. Assimilation od sea level data over continental shelves: an ensemble method for the exploration of model errors due to uncertainties in bathymetry, *Dyn. Atmos. Oceans.*, **38,** 93–121.

Padman, L. & Fricker, H.A., 2005. Tides on the Ross Ice Shelf observed with ICESat, *Geophys. Res. Lett.*, **32,** L14503, doi:10.1029/2005GL023214.

Pairaud, I.L., Lyard, F., Auclair, F., Letellier, T. & Marsaleix, P., 2008. Dynamics of the semi-diurnal and quarter-diurnal internal tides in the Bay of Biscay. Part I: barotropic tides, *Contin. Shelf Res.*, **28,** 1294–1315.

Ray, R., 1999. The GSFC ocean tide model, GOT99.2b, NASA Technical Memorandum 209478, 58 pp.

Ray, R., 2007. Propagation of the overtide M4 through the deep Atlantic Ocean, *Geophys. Res. Lett.*, **34,** L21602, doi:10.1029/2007GL031618.

Ray, R. & Luthcke, S.B., 2006. FAST TRACK PAPER: tide model errors and GRACE gravimetry: towards a more realistic assessment, *Geophys. J. Int.*, **167,** 1055–1059, doi:10.1111/j.1365–246X.2006.03229.x.

Savcenko, R. & Bosch, W., 2007. Residual tide analysis in shallow water—contribution of ENVISAT and ERS altimetry, in *Proceedings of the Envisat Symposium 2007*, ESA-SP636 (CD-ROM), eds Lacoste, H. & Ouwehand, L., ESA, Noordwijk.

Savcenko, R. & Bosch, W., 2008. EOT08a—empirical ocean tide model from multi-mission satellite altimetry, Report No.81, Deutsches Geodätisches Forschungsinstitut, München, Germany.

Schmidt, R., Meyer, U., Dahle, Ch., Flechtner, F. & Kusche, J., 2008. Monthly and weekly EIGEN-GRACE05S gravity field solutions for monitoring of mass variations in the earth system, in *Surface Water Storage and Runoff: Modeling, In-Situ Data and Remote Sensing, Proceedings of the 2nd Space for Hydrology Workshop*, ESA-SP636 (CD-ROM), eds Benveniste, J. *et al.*, ESA, Noordwijk.

Schrama, E.J.O. & Ray, R.D., 1994. A preliminary tidal analysis of TOPEX/POSEIDON alimetry, *J. geophys. Res.*, **99**(C12), 24 799–24 808.

Seo, K.W., Wilson, C.R., Han, S.C. & Waliser, D.E., 2008. Gravity Recovery and Climate Experiment (GRACE) alias error from ocean tides, *J. geophys. Res.*, **113,** B03405, doi:10.1029/2006JB004747.

Shum, C.K., Yu, N. & Morris, C., 2001. Recent advances in ocean tidal science, *J. Geod. Soc. Japan*, **47**(1), 528–537.

Simmons, H., Hallberg, R. & Arbic, B., 2004. Internal wave generation in a global baroclinic tide model, *Seep Sea Res.*, **51,** 3043–3068.

Smith, A.J.E., 1999. Application of satellite altimetry for global ocean tide modelling, *PhD thesis*, Delft Institute for Earth-Oriented Space Research, Delft University of Technology, Faculty of Aerospace Engineering.

Smithson, M.J., 1992. *Pelagic tidal constants-3*, IAPSO Publ. Sci. No. 35, IAPSO (IUGG), Gothenburg.

Taguchi, E., 2004. Inverse Modellierung nichtlinearer Flachwassergezeiten und ihre Anwendung auf ein Randmeer, *Berichte aus dem Zentrum für Meeres- und Klimaforschung*, **47**.

Wünsch, J., Schwintzer, P. & Petrovic, S., 2005. Comparison of two different ocean tide models especially with respect to the GRACE satellite mission, Scientific Technical Report STR05/08, GeoForschungsZentrum Potsdam, Potsdam.

Zahel, W., 1991. Modeling ocean tides with and without assimilating data, *J. geophys. Res.*, **96,** 20 379–20 391.

Zahel, W., 1995. Assimilating ocean tide determined data into global tidal models, *J. Mar. Syst.*, **6,** 3–13.

Zahel, W., Gaviño, J. & Seiler, U., 2000. Angular momentum and energy budget of a global ocean tide model with data assimilation. *GEOS*, **20**(4), 400–413.

Zaron, E.D. & Egbert, G.D., 2006. Estimating open-ocean barotropic dissipation: the Hawaiian ridge, *J. Phys. Oceanogr.*, **36**(6), 1019–1035.